Self-assembled monolayers of polyoxovanadates with phthalocyaninato lanthanide moieties on gold surfaces

Pütt, Ricarda; Qiu, Xinkai; Kozłowski, Piotr; Gildenast, Hans; Linnenberg, Oliver; Zahn, Stefan; Chiechi, Ryan C; Monakhov, Kirill Yu

Published in:
Chemical communications (Cambridge, England)

DOI:
10.1039/c9cc06852j

Publication date:
2019

ChemComm

COMMUNICATION

View Article Online
View Journal | View Issue

Cite this: *Chem. Commun.*, 2019, **55**, 13554

Received 3rd September 2019,
Accepted 14th October 2019

DOI: 10.1039/c9cc06852j

rsc.li/chemcomm

Self-assembled monolayers of polyoxovanadates with phthalocyaninato lanthanide moieties on gold surfaces†

Ricarda Pütt,[a] Xinkai Qiu,[b] Piotr Kozłowski,[c] Hans Gildenast,[a] Oliver Linnenberg,[a] Stefan Zahn,[d] Ryan C. Chiechi *[b] and Kirill Yu. Monakhov *[d]

The two first representatives of phthalocyaninato (Pc) lanthanide-ligated polyoxovanadate cages $\{[V_{12}O_{32}(Cl)](LnPc)_n\}^{n-5}$ (n = 1 or 2, Ln = Yb^{3+}) were synthesised and fully characterised. These magnetic complexes form two-dimensional self-assembled monolayers exhibiting electrical conductivity on gold substrate surfaces, as assessed by using an EGaIn tip.

The possibility of forming stimuli-responsive two-dimensional (2D) monolayers[1] paves the way for implementation of nanostructured molecule–surface interfaces into highly sought-after molecule-based computer memory cells. Self-assembled monolayers (SAMs) consisting of tailor-made metal complexes[2] constitute one of the promising ways of addressing the challenges[3] in the area of molecular electronics.[4,5] To transit to the actual device fabrication, experimentalists need first and foremost to achieve active control of contact-surface impacted single-molecule structure–property stability and of the reproducibility of molecular conductivity measurements. A continuous optimisation of coordination compounds is furthermore required to eventually minimise resistivity and improve the conductivity of 2D SAMs in the applied electrode environment.

Herein we report on our efforts towards the development of such SAMs whose molecular electronic states can be manipulated on air-stable substrate surfaces by electrical means and their working functions can be tracked by (micro)-spectroscopic methods. Specifically, we elaborate on polyoxovanadates[6] (POVs) and, specifically, their organic–inorganic hybrid derivatives that have been identified[7] as being able to implement multilevel data storage and processing functions in so-called "More than Moore" IT devices. We describe the synthesis, structure and magnetism of nBu$_4$N$^+$-charged balanced complexes with the general formulas $\{[V^V_{12}O_{32}(Cl)](LnPc)\}^{4-}$ (**mono**$^{4-}$) and $\{[V^V_{12}O_{32}(Cl)](LnPc)_2\}^{3-}$ (**bis**$^{3-}$) where Pc is the phthalocyanine dianion (Fig. 1). This Communication is a focused case study with Ln = Yb^{3+}, emphasising the significance of covalent grafting of late and early lanthanide–Pc moieties onto the lacunary POV core[8,9] and its far-reaching implications on molecular charge transport characteristics. To the best of our knowledge, the direct interaction between metal–Pc moieties and the polyoxometalate[10,11] (POM) unit was shown only once. Drain and co-workers synthesised[12] hybrid $(n\text{Bu}_4\text{N})_5[PW^{VI}{}_{11}O_{39}(MPc)]$ compounds where the

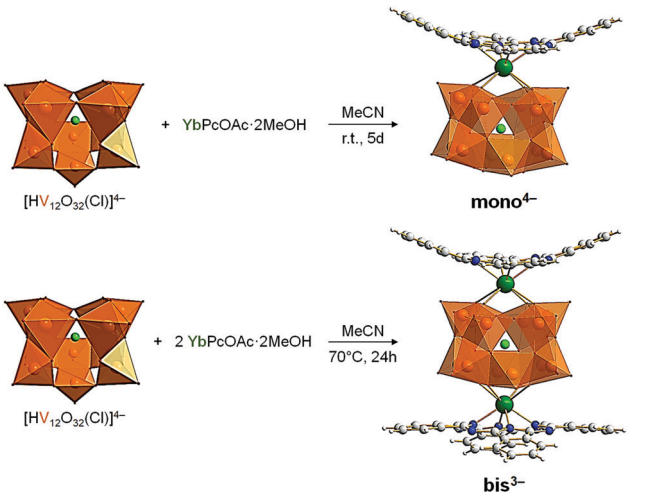

Fig. 1 Synthesis of fully-oxidised $\{[V_{12}O_{32}(Cl)](YbPc)_n\}^{n-5}$ hybrid polyanions with n = 1 (top, **mono**$^{4-}$) and n = 2 (bottom, **bis**$^{3-}$). The H^+ proton in $[HV_{12}O_{32}(Cl)]^{4-}$ is not shown. r.t. = room temperature. Colour code: Yb = dark green, V = orange polyhedra, Cl = pale green, O = red, N = blue, C = grey, and H = white. See the ESI,† for details of synthesis and crystallographic data (Table S3).

[a] *Institut für Anorganische Chemie, RWTH Aachen University, Landoltweg 1, 52074 Aachen, Germany*
[b] *Stratingh Institute for Chemistry & Zernike Institute for Advanced Materials, University of Groningen, Nijenborgh 4, Groningen 9747 AG, The Netherlands. E-mail: r.c.chiechi@rug.nl*
[c] *Faculty of Physics, Adam Mickiewicz University in Poznań, ul. Uniwersytetu Poznańskiego 2, 61-614 Poznań, Poland*
[d] *Leibniz Institute of Surface Engineering (IOM), Permoserstraße 15, 04318 Leipzig, Germany. E-mail: kirill.monakhov@iom-leipzig.de*

† Electronic supplementary information (ESI) available: Details of synthesis, analytical characterisation, magnetism and DFT calculations. CCDC 1950768 and 1950769. For ESI and crystallographic data in CIF or other electronic format see DOI: 10.1039/c9cc06852j

fully-oxidised, lacunary Keggin POM is capped by MPc^{2+} with M = Zr^{IV} or Hf^{IV}. Note that there are however plenty of hybrid compounds[13,14] where the POM unit and the metal–Pc moieties are separated by electrostatic interactions or by an organic linker.

Hybrids **mono**$^{4-}$ and **bis**$^{3-}$ were isolated as polycrystalline powders in high yields (95 and 91%) from the reactions of the $(n\mathrm{Bu_4N})_4[\mathrm{HV_{12}O_{32}(Cl)}]$ precursor with YbPcOAc·2MeOH (OAc = acetate) in a 1 : 1 and 1 : 2.2 ratio in MeCN, respectively (Fig. 1). Single-crystal X-ray diffraction studies indicated reactivity-induced changes of the POV building unit from a "closed"-to a "tube"-like $V_{12}O_{32}$ structure[15,16] that is thus capped by one (in **mono**$^{4-}$) or sandwiched by two (in **bis**$^{3-}$) $YbPc^{+}$ moieties (Fig. 1). The formal oxidation states of the vanadium and lanthanide atoms were confirmed by bond valence sum calculations [$\sum(V^{V})$ = 4.99–5.13, $\sum(Yb^{III})$ = 2.81] for **mono**$^{4-}$ and [$\sum(V^{V})$ = 4.80–5.26, $\sum(Yb^{III})$ = 2.80] for **bis**$^{3-}$. The formation, composition and electronic structure of the fully-oxidised **mono**$^{4-}$ and **bis**$^{3-}$ are furthermore supported by elemental and thermogravimetric analyses, electrospray ionisation mass spectrometry and SQUID magnetometry (for details see the ESI†).

Magnetism of both compounds arises from Yb^{3+} ions and is dominated by spin–orbit interaction. Because Yb^{3+} has a more than half-filled 4f valence shell, its ground multiplet should correspond to a high total magnetic moment $J = 7/2$.[17] Since the energy gap between the ground and the first exited multiplet in Yb^{3+} is supposed to be around 14 000 K[18] only the ground multiplet was considered in modelling of the magnetism. In Fig. 2 the molar susceptibility and magnetisation of **mono**$^{4-}$ are depicted together with theoretical fits. The details of magnetic modelling of **bis**$^{3-}$ (Fig. S12) can be found in the ESI.†

The electronic structure of **mono**$^{4-}$ was also assessed by density functional theory calculations (for details see the ESI†) and it is in line with the obtained magnetic data. As illustrated in Fig. 3, the negative charge is transferred from the Pc to the POV subunit, while a doublet spin state is strongly localised at

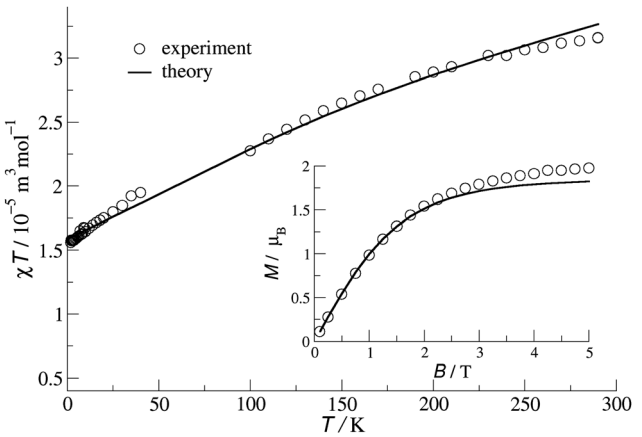

Fig. 2 Molar susceptibility (B = 0.1 T) and magnetisation (T = 2 K) for the polycrystalline powder sample of **mono**$^{4-}$ (circles) with theoretical fits (solid lines).

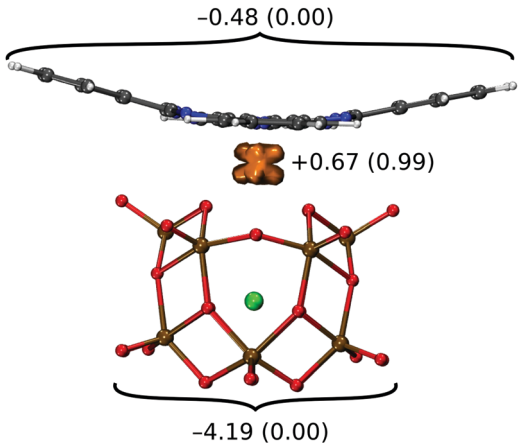

Fig. 3 Hirshfeld partial charges and regions with increased α-spin density (orange isosurface) in **mono**$^{4-}$. Sum of partial charges is shown without brackets, while the spin density is indicated in brackets.

the Yb atom. The computed Yb···Cl distance of 4.06 Å matches the experimental value of 4.1001(29) Å determined by X-ray diffraction which is *ca.* 0.34 Å longer than the one in the **bis**$^{3-}$ derivative (exptl. 3.760(2)–3.761(2) Å). This is due to the fact that the Cl atom is pushed away from Yb by *ca.* 0.21 Å in **mono**$^{4-}$ if the POV centre is taken as a reference point. The asymmetry within the POV subunit is induced by the coordinated Yb atom contracting the host–guest vanadium–oxo cluster. The largest O–O distance between the Yb-coordinated oxygen atoms is 3.99 Å (exptl. 4.0611(279) Å), and it is increased to 4.71 Å (exptl. 4.9368(85) Å) on the opposite POV side for the comparable oxygen atoms.

Next, we succeeded in growing SAMs by immersing freshly cleaved templated-stripped[19] gold substrates (atomically smooth Au^{TS}) in a ~0.1 mM methanolic solution of each tested, thermally stable (up to *ca.* 200 °C) coordination compound overnight. The formation of SAMs is shown in Fig. 4A–C. SAMs were contacted with an EGaIn[20] tip to form tunnel junctions with the structure Au^{TS}//SAM//Ga_2O_3/EGaIn, where "/" denotes the interface defined by chemisorption and "//" by physisorption. The SAM quality was assessed by measuring the morphology of the fabricated sample surfaces (Fig. 4A–C and Fig. S13 in the ESI†) using atomic force microscopy (AFM). The observed particles exhibiting the size of physisorbed **mono**$^{4-}$ and **bis**$^{3-}$ are homogeneously distributed over the Au^{TS} substrate surface (Fig. 4A and Fig. S13 in the ESI†) that is characterised by the absence of molecular aggregates (Fig. 4B). The roughness values of SAMs are estimated to be 0.417 nm for **mono**$^{4-}$ and 0.382 nm for **bis**$^{3-}$. They are thus higher than those (0.1 nm) obtained for the bare Au^{TS} substrates, suggesting that the target coordination compounds were successfully immobilised on gold. The formation of monolayers was confirmed by ellipsometric measurements of the SAM thickness, resulting in values 0.96 ± 0.07 nm for **mono**$^{4-}$ and 1.17 ± 0.07 nm for **bis**$^{3-}$ that are in excellent agreement with the expected height values (*ca.* 0.90 *vs.* 1.20 nm) for these hybrid polyoxoanions.

The measured current density–voltage (J–V) characteristics of the engineered SAMs are depicted in Fig. 4D. Interestingly,

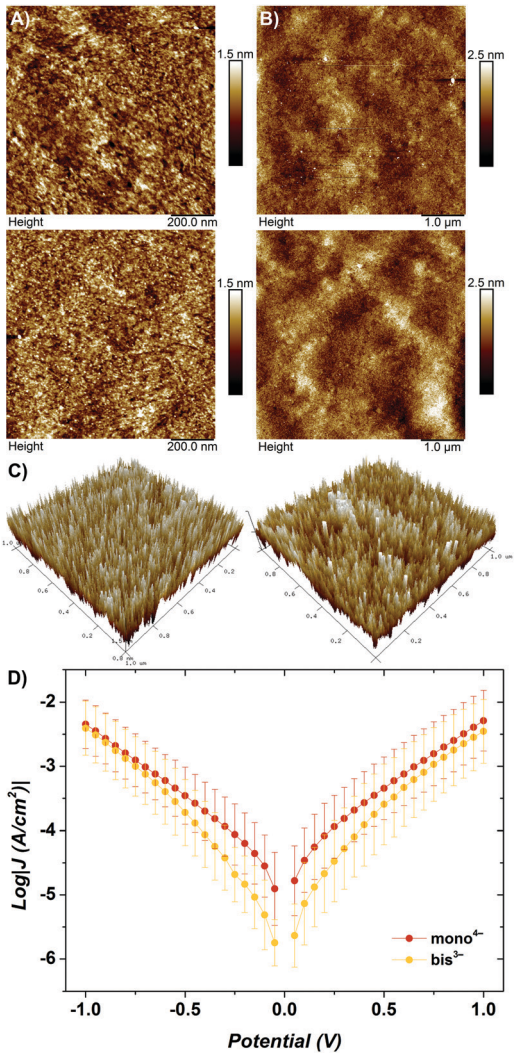

Fig. 4 AFM height images of SAMs on Au^{TS} (scanned at A) 500 µm and (B) 5 µm and the 3D morphology of the sample surfaces (C) for **mono**$^{4-}$ (top/left) and **bis**$^{3-}$ (bottom/right). (D) Plots of log current density *vs.* applied potential for SAMs of **mono**$^{4-}$ and **bis**$^{3-}$ on Au^{TS}. Values of log|*J*| at $V = 0$ V are omitted for clarity. $J = I/A$ where I and A are the current and area of the junction, respectively. Error bars represent the standard deviation of Gaussian fits.

the SAM of **bis**$^{3-}$ demonstrates somewhat lower molecular conductivity than **mono**$^{4-}$ at a low bias voltage. However, at a higher bias $\geq \pm 1$ V the difference in the rate of tunnelling charge-transport vanishes, likely due to the molecular states coming into resonance with the electrode/substrate Fermi level with the increasing bias voltage.[21] Although the magnetism of **mono**$^{4-}$ and **bis**$^{3-}$ is dominated by the spin–orbit effects of Yb^{3+} ions, the molecular charge-transport characteristics are expected to be strongly influenced by electron transport[22] through the fully-oxidised V^{V} centres. This is in accordance with our latest results[23] indicating that the Cu(II) centre is the main transmission channel across tunnel junctions formed of a series of charge-neutral dinuclear 3d–4f coordination complexes $[CuLn(L{\cdot}SMe)_2(OOCMe)_2(NO_3)]{\cdot}x$MeOH (Ln = Gd, Tb, Dy and Y; L = Schiff base; $x = 0.75$–1). The latter were similarly immobilised on Au^{TS} in the form of monolayers; however, these SAMs are characterised by lower molecular conductivity compared to the SAMs of **mono**$^{4-}$ and **bis**$^{3-}$. In view of these data, further efforts towards the grafting of covalently bound early lanthanide–Pc moieties onto (reduced) POM cores need to be devoted in order to substantially break the energy level alignment of molecular magnetic states with respect to the Fermi level of the applied electrode surfaces.

The findings described herein offer guidance to customizing a hybrid material that can be assembled of any stable lacunary POM core and phthalocyaninato lanthanide moieties. The structure-directing and -stabilising role of the charge balancing countercations is also worth mentioning.[24] A comparative analysis of the molecular charge transport characteristics of the hybrid materials and their precursors ($(n\mathrm{Bu}_4\mathrm{N})_4[\mathrm{HV}_{12}\mathrm{O}_{32}(\mathrm{Cl})]$ and LnPcOAc) will be published elsewhere. The potential possibilities of controlled fine-tuning of their structural, electrochemical and magnetic characteristics in the applied electrode environment are expected to make 2D monolayers of such POM-based coordination compounds suitable candidates for practical integration into memory cells.[25,26] To achieve this technology transfer-oriented goal, we will further seek to evoke the SAM conductivity switching response to the electric field of a scanning probe microscope as a function of oxidation and magnetic states of metal ions or temperature-controlled molecular ordering and/or adsorption geometry in monolayers.

This work was supported by the Emmy Noether program of the Deutsche Forschungsgemeinschaft (DFG). X. Q. and R. C. C. acknowledge the Zernike Institute for Advanced Materials for financial support. Computational time from the ZIH Dresden is gratefully acknowledged. Model Hamiltonian calculations were carried out at the Poznań Supercomputing and Networking Centre in Poland.

Conflicts of interest

There are no conflicts to declare.

Notes and references

1 Y. F. Yao, L. Zhang, E. Orgiu and P. Samorì, *Adv. Mater.*, 2019, **31**, 1900599.
2 S. J. Higgins and R. J. Nichols, *Polyhedron*, 2018, **140**, 25.
3 D. Xiang, X. Wang, C. Jia, T. Lee and X. Guo, *Chem. Rev.*, 2016, **116**, 4318.
4 L. Vilà-Nadal, S. G. Mitchell, S. Markov, C. Busche, V. Georgiev, A. Asenov and L. Cronin, *Chem. – Eur. J.*, 2013, **19**, 16502.
5 C. Busche, L. Vilà-Nadal, J. Yan, H. N. Miras, D.-L. Long, V. P. Georgiev, A. Asenov, R. H. Pedersen, N. Gadegaard, M. M. Mirza, D. J. Paul, J. M. Poblet and L. Cronin, *Nature*, 2014, **515**, 545.
6 M. Stuckart and K. Y. Monakhov, *Vanadium: Polyoxometalate Chemistry. In Encyclopedia of Inorganic and Bioinorganic Chemistry*, ed. R. A. Scott, 2018, pp. 1–19.
7 O. Linnenberg, M. Moors, A. Notario-Estévez, X. López, C. de Graaf, S. Peter, C. Bäumer, R. Waser and K. Y. Monakhov, *J. Am. Chem. Soc.*, 2018, **140**, 16635.
8 Y. Hayashi, *Coord. Chem. Rev.*, 2011, **255**, 2270.
9 J. M. Cameron, G. N. Newton, C. Busche, D.-L. Long, H. Oshio and L. Cronin, *Chem. Commun.*, 2013, **49**, 3395.
10 D.-L. Long, R. Tsunashima and L. Cronin, *Angew. Chem., Int. Ed.*, 2010, **49**, 1736.

11 M. Stuckart and K. Y. Monakhov, *Chem. Sci.*, 2019, **10**, 4364.
12 I. Radivojevic, K. Ithisuphalap, N. P. Burton-Pye, R. Saleh, L. C. Francesconi and C. M. Drain, *RSC Adv.*, 2013, **3**, 2174.
13 Y. Yang, L. Xu, F. Li, X. Du and Z. Sun, *J. Mater. Chem.*, 2010, **20**, 10835.
14 X. Song, R. Liu, Z. Sun, H. Shi and L. Xu, *Mater. Res. Bull.*, 2018, **97**, 326.
15 Y. Inoue, Y. Kikukawa, S. Kuwajima and Y. Hayashi, *Dalton Trans.*, 2016, **45**, 7563.
16 S. Kuwajima, Y. Ikinobu, D. Watanabe, Y. Kikukawa, Y. Hayashi and A. Yagasaki, *ACS Omega*, 2017, **2**, 268.
17 J. Jensen and A. R. Mackintosh, *Rare earth magnetism: structures and excitations*, Clarendon Press, Oxford, 1991.
18 G. H. Dieke, *Spectra and Energy Levels of Rare Earth Ions in Crystals*, Wiley, New York, 1968.
19 E. A. Weiss, G. K. Kaufman, J. K. Kriebel, Z. Li, R. Schalek and G. M. Whitesides, *Langmuir*, 2007, **23**, 9686.
20 W. F. Reus, M. M. Thuo, N. D. Shapiro, C. A. Nijhuis and G. M. Whitesides, *ACS Nano*, 2012, **6**, 4806.
21 Y. Zhang, S. Soni, T. L. Krijger, P. Gordiichuk, X. Qiu, G. Ye, H. T. Jonkman, A. Herrmann, K. Zojer, E. Zojer and R. C. Chiechi, *J. Am. Chem. Soc.*, 2018, **140**, 15048.
22 M. Laurans, K. Dalla Francesca, F. Volatron, G. Izzet, D. Guerin, D. Vuillaume, S. Lenfant and A. Proust, *Nanoscale*, 2018, **10**, 17156.
23 S. Schmitz, A. Kovalchuk, A. Martín-Rodríguez, J. van Leusen, N. V. Izarova, S. D. M. Bourone, Y. Ai, E. Ruiz, R. C. Chiechi, P. Kögerler and K. Y. Monakhov, *Inorg. Chem.*, 2018, **57**, 9274.
24 A. Misra, K. Kozma, C. Streb and M. Nyman, *Angew. Chem., Int. Ed.*, 2019, DOI: 10.1002/anie.201905600.
25 K. Y. Monakhov, M. Moors and P. Kögerler, Polyoxometalate Chemistry, in *Adv. Inorg. Chem.*, ed. R. van Eldik and L. Cronin, Academic Press, Elsevier, *Amsterdam*, 2017, vol. 69, p. 251.
26 X. Chen, Y. Zhou, V. A. L. Roy and S.-T. Han, *Adv. Mater.*, 2018, **30**, 1703950.